ELECTROCHEMICAL EVALUATIONS OF HIGH SHEAR CORROSION INHIBITORS USING JET IMPINGEMENT

C. M. Menendez, S. J. Weghorn and Y. S. Ahn
Baker Petrolite Corporation
12645 W. Airport Blvd.
Sugar Land, Texas 77095
USA

A. Jenkins and W. Y. Mok
Baker Petrolite
Kirkby Bank Road
Knowsley Industrial Park
Liverpool
L33 7SY
UK

ABSTRACT

Corrosion inhibitors are required to provide adequate protection in CO2 and/or H_2S environments operated under high wall shear stress conditions. Jet impingement test methodology is used in this paper to study the flow-accelerated corrosion under extremely high shear stress conditions. This study is focused on the methodology aspects of using the jet impingement coupled with a new localized corrosion monitoring (LCM) technique for the selection of corrosion inhibitors for high shear applications with emphasis on localized corrosion. LCM technique and its data analysis program were employed to identify the occurrence of localized corrosion events as well as its magnitude, duration, frequency and distribution. A number of sulfur-containing corrosion inhibitors were evaluated using the new test methodology.

Keywords: jet impingement, localized corrosion, corrosion inhibitors, localized corrosion monitoring (LCM), wall shear stress, sulfur compounds.

INTRODUCTION

The use of corrosion inhibitors to control internal corrosion of carbon steel structures in oil and gas production facilities is a well established industrial practice adopted by the industry. The typical approach in selecting a corrosion inhibitor for a specific application is via series of laboratory screening tests to determine the inhibition capability of candidate chemicals under a specific set of test conditions. The preliminary performance tests undertaken may include wheel test, kettle tests and partitioning tests[1-3]. Additional tests may then be conducted to simulate more closely the field operating conditions, such as high pressure, high temperature and high wall shear stress, etc. In such cases, more specialized tests can be performed using more complex equipment, such as rotating cylinder electrode (RCE), high shear autoclave (HSAT), flow loop and jet impingement equipment[4-6], etc.

The evaluation of corrosion inhibitor performance is traditionally based on weight loss measurements and/or electrochemical monitoring, such as linear polarization resistance (LPR) measurements, which provide information on the general corrosion rate. With coupon exposure tests, localized corrosion information may also be obtained, provided the duration of the exposure test is sufficient long to enable pits to be fully developed, which may take weeks or even months depending on the test conditions.

In high flow rate high shear stress operating environment, a number of corrosion inhibitors containing sulfur based compounds have been developed for this type of applications. Two of such sulfur based compounds are thioglycolic acid (TGA) and mercaptoalcohol (MA), which were reported to give good performance in high shear tests[7, 8]. Although corrosion inhibition performance tests on both types of chemistry suggested that the overall general corrosion rate was low, there was also some experimental evidence suggesting that the presence of TGA might lead to localized attack in RCE tests; whereas MA containing inhibitors exhibited superior pitting corrosion inhibition behavior[9].

As field experience suggested that localized corrosion is a major cause of pre-mature failure[10], this leads to a conclusion that not all inhibitors are effective in controlling localized corrosion. In some applications, the use of certain types of corrosion inhibitors could even promote localized corrosion[11-13]. It is therefore very important to characterize the effectiveness of candidate corrosion inhibitors in minimizing not just general corrosion, but also their effectiveness in controlling localized corrosion.

The recent development of corrosion monitoring techniques has provided a tool to detect the occurrence of localized corrosion behavior[14, 15]. One of the electrochemical monitoring techniques is Localized Corrosion Monitoring (LCM). This paper presents the results of using both LPR and LCM in jet impingement tests to evaluate the performance of two corrosion inhibitors, one containing MA and the other containing TGA. The uses of jet impingement equipment allowed tests to be conducted under more severe test conditions, i.e. higher shear stress such that a better assessment of the performance of the 2 chemicals in controlling both general and localized corrosion could be made.

EXPERIMENTAL

Materials

The corrosion inhibitors studied consisted of two (2) identical corrosion inhibitor formulations that only differed in the type of sulfur compounds employed. The first compound was a proprietary mercaptoalcohol (MA) whereas the second was thioglycolic acid (TGA). The later was obtained from commercially available sources.

Corrosion Environment

The testing fluid consisted of a synthetic brine/hydrocarbon (90:10) mixture at 140°F. The synthetic brine composition is given in Table 1. The hydrocarbon employed for testing was Isopar M™. The tests were conducted at a CO_2 partial pressure of 14.5 psi.

Jet Impingement Measurements

The jet impingement measurements were conducted using a setup resembling the one reported by Efird[16]. According to this design the test probe and the jet are aligned horizontally and while the fluids discharge takes place through the top of the cell. The test probe employed in the present paper included the auxiliary and the working electrodes only. In this case the probe surface facing the jet consisted of a single working ring electrode. The reference electrode employed was a 3 mm bar made from Alloy 276 material. The reference electrode was installed in a separate port of the testing chamber. A similar jet impingement cell was also reported by Macdonald et al[17].

The distance between the jet and the working ring was set at 4 mm for all experiments. The C1018 working ring was located in the wall jet region in accordance with the work of Giralt and Trass[18]. The equation employed to calculate the wall shear stress as a function of flow and geometry is given below:

$$\tau_W = 0.0447 \rho V_0^2 \, \mathrm{Re}^{-0.182} \left(\frac{x}{D}\right)^{-2} \qquad (1)$$

In the given equation, τ_W, is the wall shear stress (Pa), ρ is the fluid density (Kg/m^3), D is the diameter of the jet (m), V_0 is the velocity of the fluid at the outlet of the jet (m/s), x is the radial distance from the jet's center line (m), Re is the Reynolds number based on the dimensions of the jet (Re=Vo.D/ν), ν is the kinematic viscosity (m^2/s).

Localized Corrosion Monitoring (LCM)

An ACM Instruments unit was employed for the LCM measurements. In a typical LCM experiment, both potential and current are alternatively recorded with time using 30 seconds on (current) and 30 seconds off (potential) potentiostatic control/open circuit potential sequence. The general corrosion rates were calculated using an option available in the analysis software. To calculate a corrosion rate based on the LCM measurements the software will determine the standard deviation of potential and current records first. The calculated standard deviations are then used to calculate the corrosion resistance which in turn is used to calculate the corrosion rate the same way as in LPR. The Stern-Geary constant (B) employed to calculate the corrosion rate both for LPR and the noise measurements was of 0.026 mV.

Test Procedure

The testing fluids were sparged with CO_2 to remove oxygen and loaded into the jet impingement apparatus under positive pressure. The electrochemical measurements were started on an already inhibited surface (no pre-corrosion was allowed). This was accomplished by adding 200 ppm of corrosion inhibitor to the fluids before the probe was allowed to expose in the test environment.

The short term LCM measurements were conducted starting from a wall shear stress of 100 Pa for half an hour. The shear stress was subsequently increased to 500 and 700 Pa every one and half hours. The long term LCM measurements were conducted in a similar way but at a maximum shear stress of 500 Pa. In this case the working ring was exposed to the environment for 15 hours. At the end of the

experiment the surface of the working ring was subjected to microscopic examination using Nikon Eclipse ME600 optical microscope.

RESULTS AND DISSCUSION

LCM Potential/Current Transient Analysis

The LCM potential/current analysis employed in this paper follows the description given by Mok et al.[19] In a typical LCM experiment, both potential and current are alternatively recorded with time using 30 seconds on (current) and 30 seconds off (potential) potentiostatic control/open circuit potential sequence. LCM relies on the measurements of time of occurrence, magnitude, duration, frequency and distribution of distinct potential (negative) and current (positive) transients as a result of initiation and/or propagation/repasivation of localized corrosion events (e.g. pitting, crevice). Based on the magnitude, duration and relative rate of decrease/increase of potential and current signals, four different types of transients can be observed in the LCM time records: (i) initiation/propagation (IP), (ii) initiation/partial repassivation (IPR), (iii) initiation/repassivation (IR) and (iv) initiation/repassivation/propagation (IRP) transients are observed. This transient analysis of the potential/current time dependence will be used in quantifying localized corrosion activity on the carbon steel and stainless steel tests.

Type I: Potential IP transients are characterized by a sudden decrease in open-circuit potential, i.e. pit initiation (1-3 sec), followed by a slow increase in potential (typically > 30 sec), i.e. pit propagation, close to or lower than its original value. The typical decrease in potential is < 3 mV. The corresponding current transients, whether preceding or following the potential transients can vary significantly depending on the localized corrosion activity (0.1 – 100 μA). The lower the ratio of the magnitudes of potential and current transients (Rt), the more active the pit and greater the area affected. A typical potential/current IP transient is presented in Figure 1a showing sharp decrease (pit initiation) and subsequent slow increase (pit propagation) in potential accompanied with the current peak. Pits that grow by this mechanism are generally most active, non-uniformly distributed, large and deep (see discussion on corrosion inhibitor).

Type II: Potential IPR transients can be described in terms of sudden, decrease in open-circuit potential (typically < 3 mV) followed by a slow increase in potential to, higher or lower than the initial open-circuit potential. These transients can extend over much larger time periods (> 1000 sec) compared to the potential IP transients. The corresponding current transients show both larger current initiation (increase) and lower current partial repassivation (decrease) signals. The typical current increases during these transients are < 10 μA. Figure 1b depicts one of the IPR potential/current transients showing pit initiation/partial repassivation. Pits formed by the IPR mechanism are generally active, more uniformly distributed, smaller and more shallow (see discussion on corrosion inhibitors).

Type III: Potential IR transients can be characterized by a rapid and generally larger decrease in potential (2-100 mV) associated with an equally fast increase in potential to its original value within few free potential/potential hold cycles. The corresponding current transients (<1-2 μA) show equally strong positive (initiation) and negative (passivation) signals (Figure 1c). Typical IR transients are associated with passive, numerous, uniformly distributed extremely small pits (see discussion on stainless steel in NaCl).

Type IV: Potential IRP transients can be described in terms of a steady and large decrease in potential (10-50mV) followed by a slow increase in potential to a level that is significantly lower than the initial open-circuit potential. These potential transients extend over much larger time periods 1-10 cycles)

compared to the potential IP, IPR and IR transients. The IRP current transients show generally successive repassivation and propagation associated with multiple localized corrosion events. Figure 1d depicts one of the IPR transients showing pits initiation/repassivation and continuous propagation of certain number of them. Pits formed by the IPR mechanism are generally in very large number, more or less active, uniformly distributed, smaller and more shallow than the IP and IPR (see discussion on corrosion inhibitors).

Short-Term Test

Figure 2a and 2b shows the LCM general corrosion rate results obtained for two sulfur containing inhibitors, mercapto alcohol (MA) and thioglycolic acid (TGA), respectively. Three levels of wall shear stress were employed in the tests. The test was started with a shear stress of 100 Pa during the first half hour. The remaining two segments were corrosion rate data obtained at shear stresses of 500 and 700 Pa respectively, each lasting 1.5 hours. Under a shear of 100 Pa, the corrosion rates exhibited values around 0.5 mm/year. Both formulations exhibited corrosion rates in the 0.2 mm/year range after the wall shear stress was increased to 500 Pa and remained at this low level even a higher shear stress of 700 Pa. On the basis of corrosion rate measurements alone, the results did not reveal any major differences between the two formulations regarding inhibition performance under high shear conditions. Both formulations exhibited very similar general corrosion performance.

The length of the tests presented in Figure 2 is typical of jet impingement tests to compare the relative performance of chemicals in the laboratory in terms of general corrosion rates. Localized corrosion measurements are generally not considered in assessing the overall corrosion inhibitor performance when selecting chemicals for high shear applications. Microscopic examination of metal samples after a short-term test is often not sensitive enough to detect minor localized corrosion (e.g. pitting) and consequently, short term exposure usually doesn't provide evidence of localized attack. In order to fully evaluate the capability of corrosion inhibitors, quantitative measurement of localized corrosion is needed.

In this set of tests, LCM transient analysis of the potential/current time records was also performed to provide information about the localized corrosion performance of the chemicals. Figures 3 and 4 show potential and current records for the MA - and TGA - based inhibitors, respectively. The corrosion potential in the presence of MA (Figure 3) exhibited a total shift of about 60 mV toward the anodic direction after increasing shear stress from 100 up to 500 Pa. In this case, the corrosion potential finally stabilized at values around -280 mV.

In Figure 4, the corrosion potential in the presence of TGA exhibited a larger shift of 150 mV for a similar increase of the wall shear stress. Similar results were reported in an earlier study[9] where the authors found a stronger anodic shift for TGA- as compared to MA-based inhibitor in the RCE tests. The aforementioned study indicated that MA is predominantly a cathodic inhibitor that adsorbs onto the iron carbonate/oxide film interfering with the proton reduction, while TGA is mainly an anodic inhibitor that strengthens the protective film by absorption thereby reducing iron dissolution.

The current records shown in Figures 3 and 4, showed similar patterns until an increase of shear stress from 100 to 500 Pa. Remarkable differences were observed between the two inhibitors under the wall shear stresses of 500 and 700 Pa. As shown in Figure 3, the current records obtained for the MA based formulation exhibited frequent anodic as well as cathodic transients (peaks). This type of current pattern indicates the ability of the inhibitor to promote repassivation. In contrast, the current records shown for the TGA based formulation (Figure 4) showed a series of anodic activation events without

corresponding cathodic repasivation events (cathodic peaks). The remarkable differences found in the activation/repasivation behavior of the tested formulations suggest that the formulation based on MA exhibited superior inhibition property against localized corrosion.

Figure 5 shows a sample of the potential and current records obtained for the MA based formulation. A close look at the potential records revealed that the majority of the transients were representative of the Type III (initiation/repasivation event), see Figure 1. This type of transient is characterized by a rapid and generally larger decrease in potential (2-100 mV) associated with an equally fast increase in potential to its original value within few (or one) free potential/potential hold cycles. The IR transients shown on the potential record always feature drastic decreases and increases in potential producing characteristic square-shaped transients. The analysis of the corresponding current record revealed the anodic and cathodic peaks associated with each of the events shown on the potential record.

Figure 6 shows a sample of the potential and current records obtained for the TGA based formulation. Examination of the potential record s revealed the presence of three types of potential transients. Type I transients (initiation/propagation) were the predominant mode of activity during the monitoring period. A typical example of Type I transient is shown in Figure 7, with which the potential profile featured a transient of fast initiation followed by slow recovery. The corresponding current record shows an IP transient depicted by an anodic peak. There was no indication of repassivation on neither the potential nor current data.

The potential records shown in Figure 6 also show Type II (initiation/partial repasivation, IPR) and Type IV (initiation/repasivation/propagation transient, IRP) events, respectively. The IPR transients are characterized by large initiation and slow repassivation. Pits associated with the IPR feature are generally active, more uniformly distributed, and shallow. The IPR transient showed an amplitude of about 8 mV and a recovery time of about 500 seconds which denotes slow recovery of the corrosion potential. It should be noted that the current signals observed in this case exhibited large amplitude for the initiation event and a much lower amplitude for the repasivation event. The IRP transient featured a significant potential decrease of about 30 mV (initiation event) which was followed by a slow recovery of the corrosion potential. The aforementioned transient extended for a period much longer than 10 measurement cycles. As mentioned earlier, pits formed by the IRP mechanism are generally in very large number, more likely to be uniformly distributed, smaller and shallower than the IP and IPR.

The data suggest that TGA-based formulation is likely to induce localized corrosion, while MA-based formulation is likely to provide inhibition of localized corrosion under high shear conditions. The micrographs of the metal coupons obtained after the short-term exposure to the two inhibitor solutions showed no significant pitting activity.

Long-Term Test

Longer term exposures were conducted in order to gather microscopic confirmation of the electrochemical test results obtained based on the LCM transient analysis in the short term tests. Some antecedents of localized corrosion phenomena for TGA have been reported. Jovancicevic et al.[9] reported localized corrosion phenomena produced by TGA at a dosage of 10 ppm based on a microscopic study of the electrodes from RCE tests. The TGA treated surface showed significant amounts of localized corrosion clustered around the polishing lines, while MA treated surface showed substantially less pitting. It should be noted that in the aforementioned study the localized corrosion observed was rather superficial.

Figures 8 and 9 show the potential and current records obtained for the MA and TGA based formulations in the longer duration exposure tests. The current records of the MA formulation test (Figure 8) showed the presence of activation and passivation transients during the first four hours of exposure test at a wall shear stress of 500 Pa. A period of apparent anodic activity was noted toward the end of the exposure (9 to 15 hours). This increased anodic activity is however related to the trending of the corrosion potential toward the cathodic direction. A detailed examination of the potential records during this time shows mainly general corrosion activity (no characteristic transients). In contrast, the current records shown on Figure 9 for the TGA formulation exhibited significant activation transients. The potential records showed large potential transients which can be assigned to Type IV potential/current transients.

Figure 10 shows an expanded period of potential and current records for the long duration test treating with the MA based formulation. In this case the potential records showed patterns resembling the behavior described earlier in the short-term test (Figure 5). In this case again, most of the transients observed exhibited Type III (IR) features. All the IR transients indicated in Figure 10 featured fast initiation and repasivation events which was consistent with the behavior observed in the short term test. The potential records shown on Figure 10 showed also a Type II transient. This transient exhibited an amplitude of about 10 mV followed by the slow recovery of the corrosion potential to a value quite distant from the value preceding the activation event. The current records showed a sequence of anodic and cathodic profiles suggesting a process of initiation/passivation taking place on the surface of the electrode. Figure 11 shows the only pit found on the surface after the microscopic examination. The pit found was shallow and exhibited a depth of < 5 μm. It is likely that the pit shown on the photograph was associated with the IPR event observed.

Figure 12 shows another expanded period of the potential and current recorded during the long term exposure test with TGA based formulation. The potential records show three Type IV (IRP) transients which, as mentioned earlier, feature large amplitudes of potential activation and subsequent repassivation/propagation taking place during several potential/current cycles. The potential records in this case showed the predominance of anodic events (signals). These types of transients are likely to associate with shallow pits of large number evenly distributed on the metal surface. Figure 13 shows an image of the appearance of the pitting attack found on the electrode surface after conducting microscopic examination. The micrograph also shows the presence of clusters of individual pits that had already merged. The depth measurements conducted in that particular sample showed individual pits of less than 2 μm and larger clusters with depths greater than 5 μm.

Summary of Results

The results obtained show different potential/current transient pattern behavior for two corrosion inhibitors. The two formulations only differed in the type of sulfur-containing compound employed. Early work conducted by Jovancicevic et al.[9] reported that TGA was more susceptible to pitting. However, the authors reported data corresponding only to the treatment with single component. In the present work, the results revealed similar trends but this time corrosion inhibitor formulations were employed. These results suggest that TGA had a significant influence on the pitting corrosion behavior.

The results shown above also suggest that short term assessments conducted based on LPR data may suggest strong performance of a chemical from a general corrosion stand point. However, the influence of a chemical in inducing localized corrosion must also be qualified. The LCM transient analysis results show that the appropriate identification and characterization of the transients present on the potential/current LCM records may lead to a more comprehensive assessment of the performance of a

particular chemical. In the later case the measurement technique provides information related to both general and localized corrosion. Another advantage for the LCM measurement is that an objective performance evaluation in just few hours of exposure (3 to 4 hours) can be made and thus negating the requirement of longer testing in order to result in appreciable metal loss to enable the detection of pitting damage by microscopic examination. The early detection of localized activity is particularly important in field monitoring as appropriate control measurements can be implemented to minimize the risk of premature failure.

CONCLUSIONS

1. A corrosion inhibitor formulation based on a mercaptoalcohol (MA) performed better than a similar formulation but based on thioglycolic acid (TGA). The TGA based formulation exhibited poor localized corrosion performance under high shear conditions which was identified by LCM transient analysis and microscopic examination.

2. Two corrosion inhibitor formulations that differed only in the type of sulfur compound employed exhibited remarkably different LCM transient patterns. The TGA based formulation exhibited a predominance of propagating localized corrosion events whereas the MA formulation exhibited patterns indicative of activation/repassivation.

3. The LCM analysis showed that an inhibitor performance assessment based only on LPR measurements can lead to poor selection of corrosion inhibitors for high shear applications.

4. Jet impingement measurements under high shear stress conditions in conjunction with the LCM transient analysis allowed an assessment of the localized corrosion performance of corrosion inhibitors to be made within the time frame of a short term test (three to four hours).

5. The results suggested that presence of TGA played an important role in promoting localized corrosion when used in a formulated product.

6. Both formulations exhibited good general corrosion performance up to wall shear stresses of 700 Pa.

ACKNOWLEDGEMENT

The authors wish to express their thanks to the Baker Petrolite Corporation staff for their support and encouragement during the preparation of this work.

REFERENCES

1. J. Bown and D. Harrop, “The Selection of Inhibtors for Crude Oil Pipeline”, Paper presented at Conference of Chemical Treatment in the Oil and Gas Industry, London, 1986.

2. M. Prodger, “Corrosion Inhibition selection Procedures”, Proceedings of Oilfield Chemicals E7192, Aberdeen, May 1992.

3. S. Webster, A.J. McMahon, D.M.E. Paisley and D. Harrop, “Corrosion Inhibitor Test Methods”, Sunbury Report No. ESR 95.ER.054, November 1996.

4. J.A. Dougherty, S. Ramachandran and B. Short, "Does Shear Stress have an effect on Corrosion in Sour Gas Production?", Paper No. 1069, CORROSION/2001, Houston, TX, 2001.

5. G. Schmitt, T. Simon and R.H. Hausler, "CO_2 Erosion Corrosion and its Inhibition under Extreme Shear Stress I, Development of Methodology", Paper No. 22, CORROSION/90, Las Vegas, Nevada, 1990.

6. A.E. Jenkins, W.Y. Mok, C.G. Gamble and S.R. Keenan, "Recent Advances in the Development of Environmentally Friendly Corrosion Inhibitors for Oil and Gas Systems", Paper presented at the 10th Middle East Corrosion Conference, Bahrain, March 2004.

7. T. E. Pou and S. Fouquay, "Sulphydryl and Imidazoline Salts as Inhibitors of Carbon Dioxide Corrosion of Iron and Ferrous Metals", WO Patent Application 98/41673.

8. Y.S. Ahn and V. Jovancicevic, WO patent Application 98/41673.

9. V. Jovancicevic, Y.S. Ahn, J.A. Dougherty and B.Alink, "CO_2 Corrosion Inhibition by Sulfur-Containing Organic Compounds", Paper 007, CORROSION/2000, Houston, TX, 2000.

10. Y.M. Gunaltun and T. Chevrot, "Requirements for Inhibition of Localized Corrosion", Paper No. 6, CORROSION/99, San Antonio, TX, 1999.

11. G. Cragnolino and O.H. Tuovinen, "The Role of Sulfate Reducing and Sulfur Oxidizing Bacteria on Localized Corrosion", Paper No. 244, CORROSION/83, Houston, TX, 1983.

12. T.E. Pou and J.L. Crolet, "Sensitivity of Oilfield Corrosion Inhibitors to Traces of Thiosulfate", Proc. 8th European Symposium on Corrosion Inhibitors, Ann. Univ. Ferrara, N.S., Sez. V, Suppl. 10, 1995.

13. J.L. Crolet and M.F. Magot, "Observations of Non SRB Sulfidogenic Bacteria from Oilfield Production Facilities", Paper No. 188, CORROSION/95, Houston, TX, 1995.

14. D.A. Eden, D.G. John and J.L. Dawson, WO Patent 87/07022, 1987.

15. V. Jovancecivic, US Patent 6,280,603.

16. K. D. Efird, "Jet Impingement Testing for Flow Accelerated Corrosion", Paper No.52, Corrosion 2000, NACE International, Houston, Texas.

17. H. Q. Quiroga Becerra, C. Retamoso and D. D. Macdonald, "The Corrosion of Carbon Steel in Oil-in-Water Emulsions under Controlled Hydrodynamic Conditions", Corrosion Science, Vol.42, No.3, p.561, 2000.

18. F. Giralt and O. Trass, "Mass Transfer from Crustalline Surfaces in a Turbulent Impinging Jet, Part 2: Erosion and Diffusional Transfer", The Canadian Journal of Chemical Engineering, Vol.54, June, 1976.

19. W. Y. Mok, J. A. M. de Reus, and V. Jovancicevic, "Direct Assessment of Localized Corrosion using Localized Corrosion Monitoring Technique", Paper No.053341 (this conference).

TABLE 1

Water Chemistry

Ion	g/L
Chloride	18.4
Sulfate	0.11
Calcium	0.28
Magnesium	0.2
Bicarbonate	2.75
Potassium	0.13
Strontium	0.01
Bromide	0.09

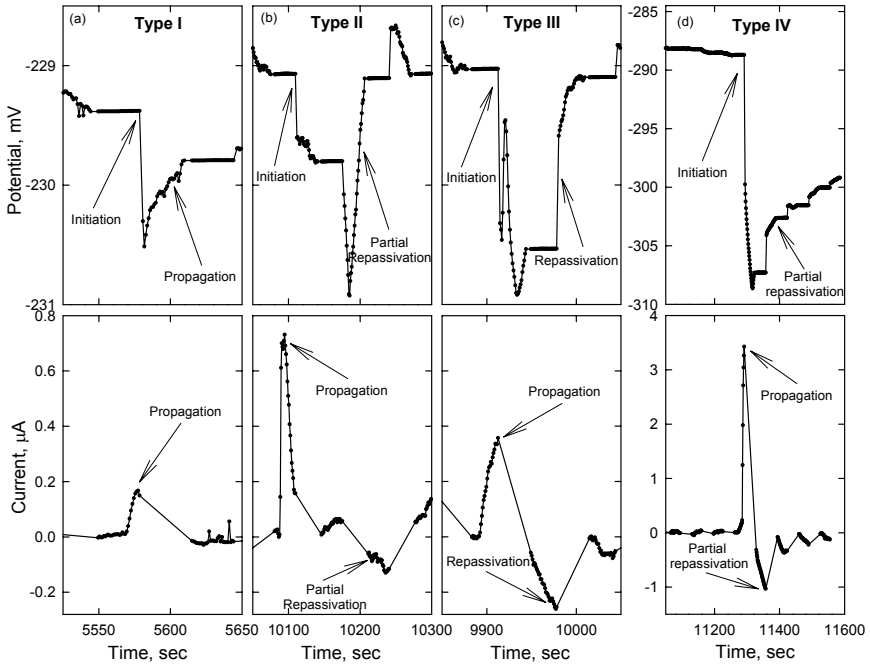

Figure 1. Four characteristic potential/current transients for pit (a) initiation/propagation (IP transients), (b) initiation/partial repassivation (IPR transients), (c) initiation/repassivation (IR transients) and (d) initiation/repassivation/propagation (IRP transients).

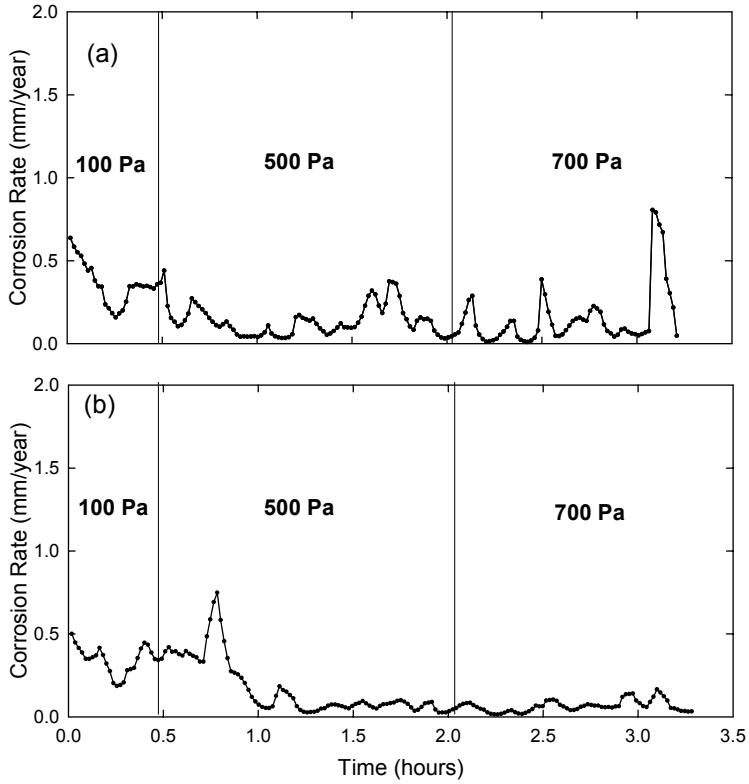

Figure 2 – Short term LCM corrosion rate results obtained for two (2) formulations: a) Formulated with MA b) Formulated with TGA.

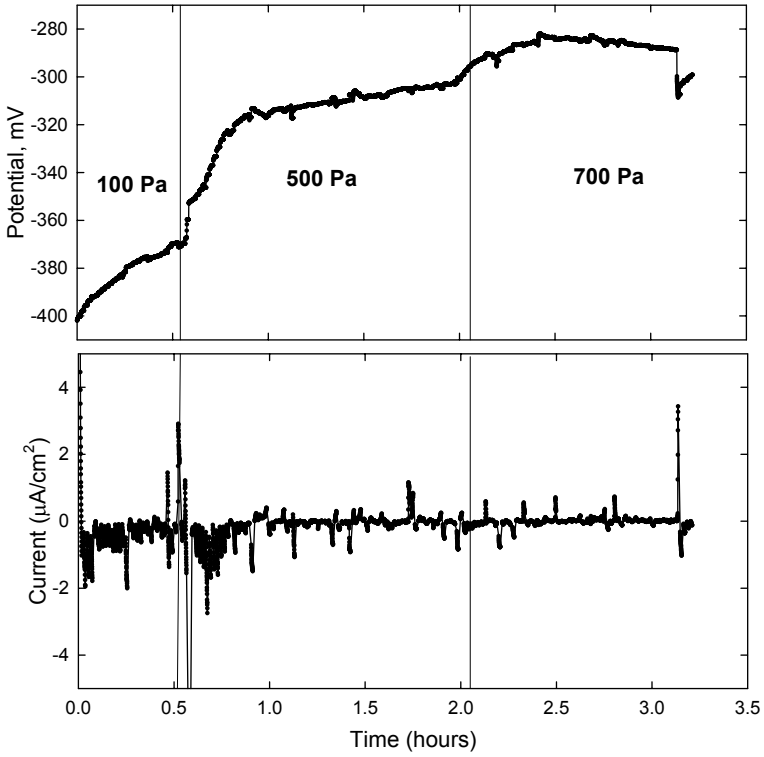

Figure 3 – Short Term LCM potential and current records for MA formulation

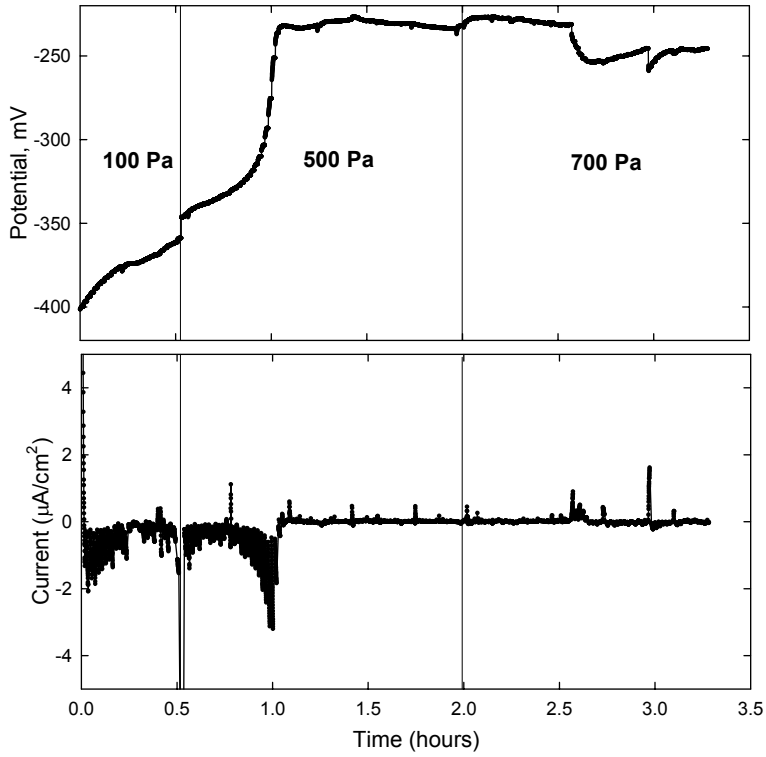

Figure 4 – Short term LCM potential and current records for TGA formulation.

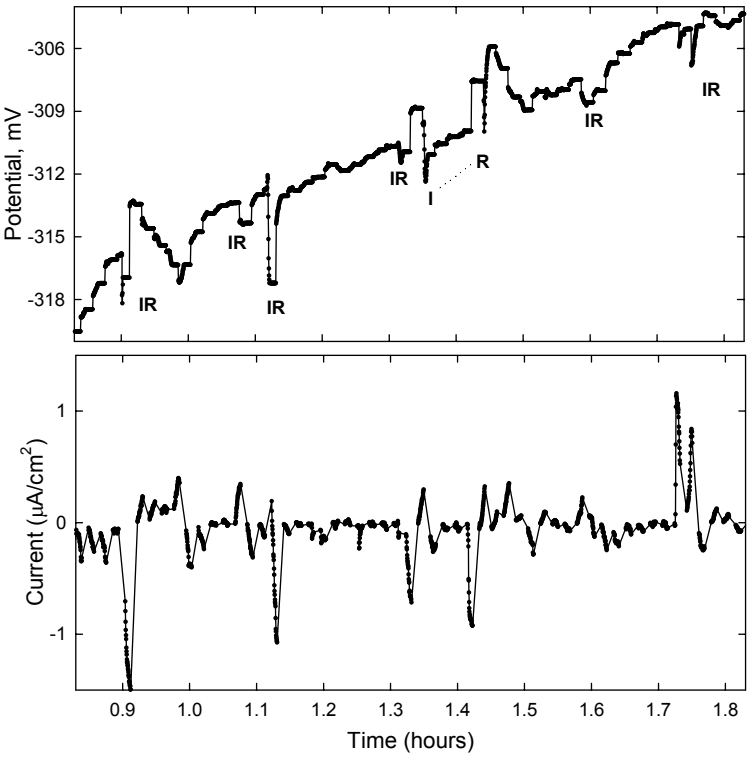

Figure 5 – Sample of short term LCM potential and current records for MA formulation.

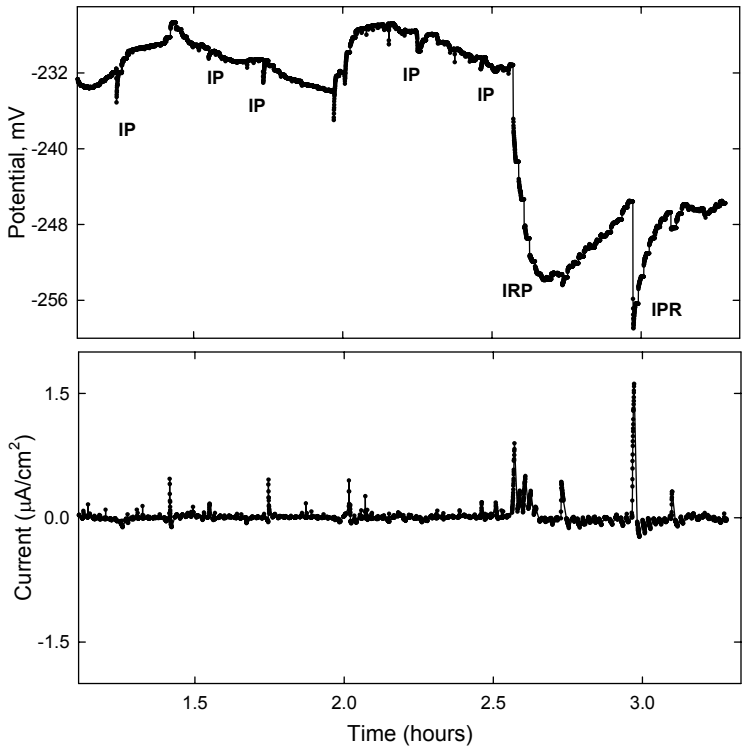

Figure 6 – Sample of short term LCM potential and current records for TGA formulation

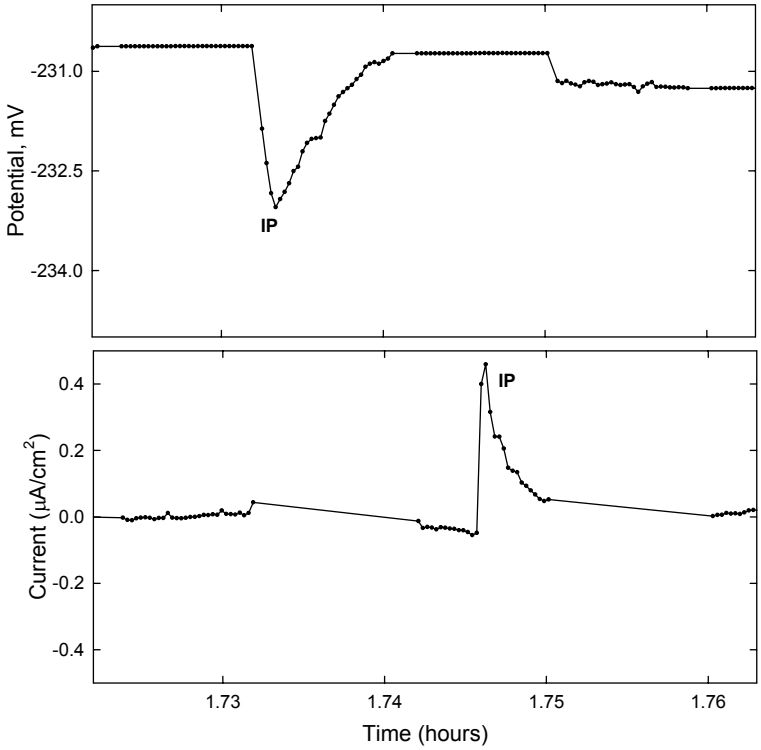

Figure 7 – Examples of IP transients extracted from short term LCM results for TGA.

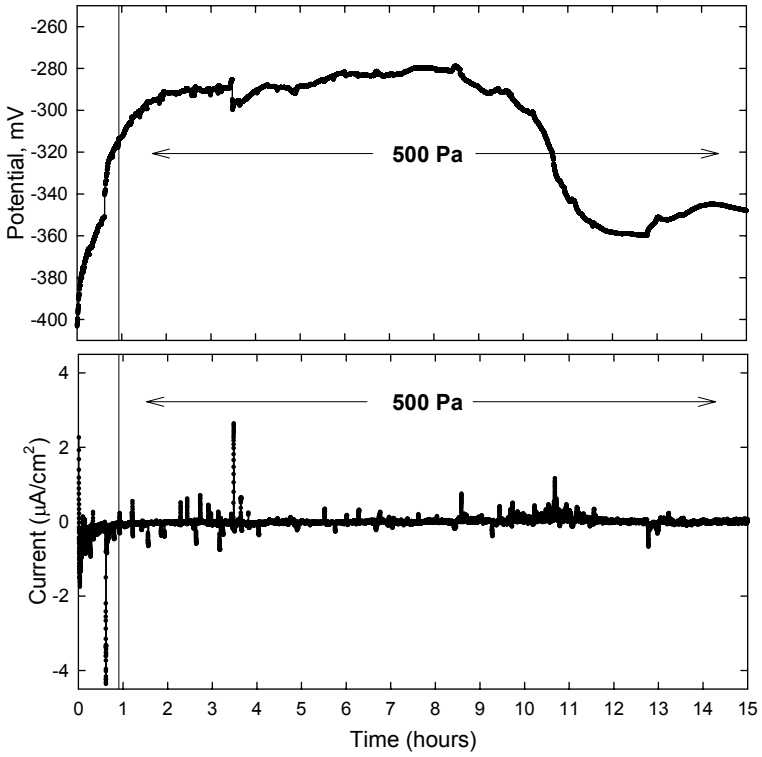

Figure 8 – Long term LCM potential and current records for MA formulation.

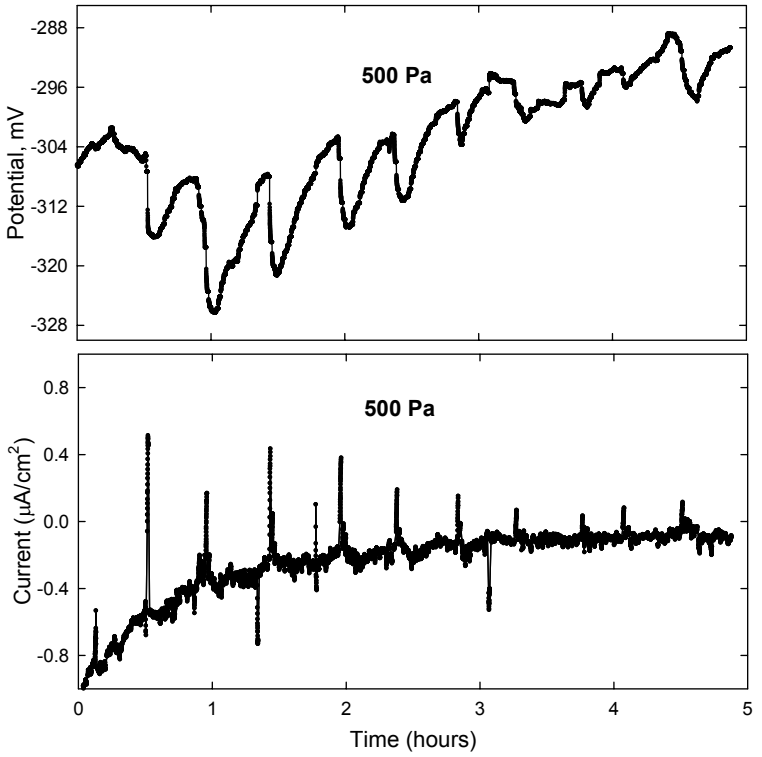

Figure 9 – Long term LCM potential and current records for TGA formulation.

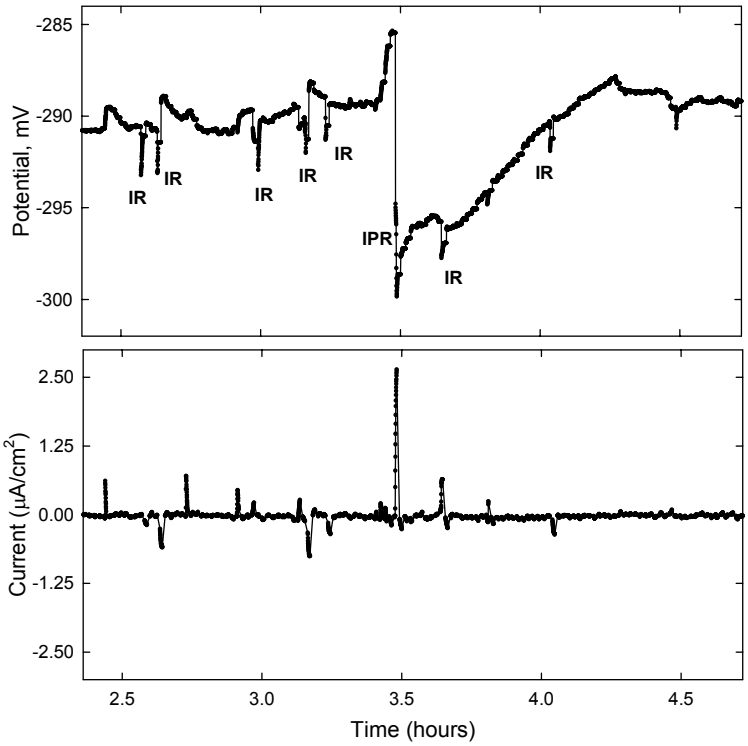

Figure 10 – Sample of LCM potential and current records from long term results for MA formulation

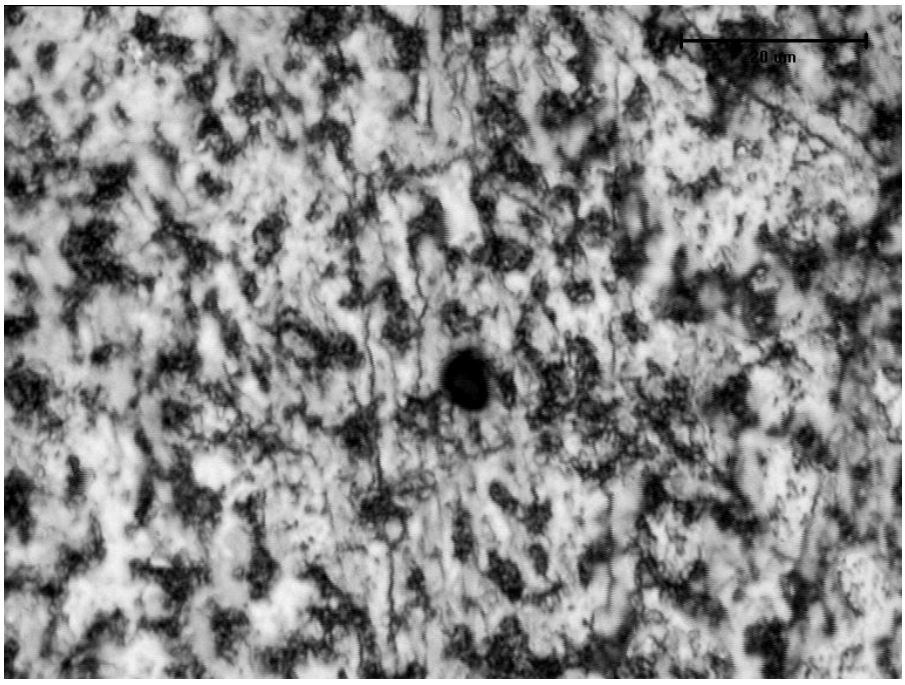

Figure 11 – Pit found after long term treatment with MA formulation (X50)

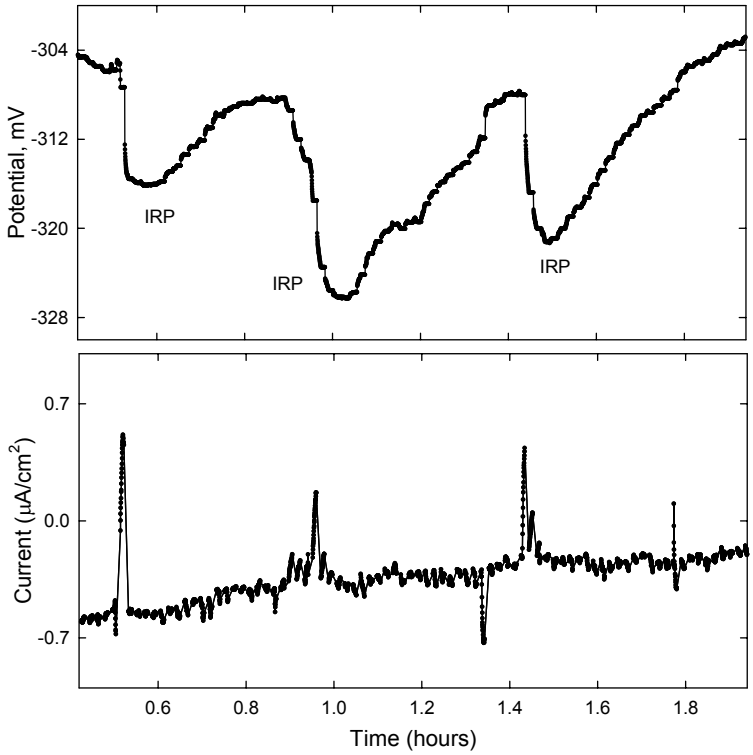

Figure 12 – Sample of long term LCM potential and current records extracted from TGA results.

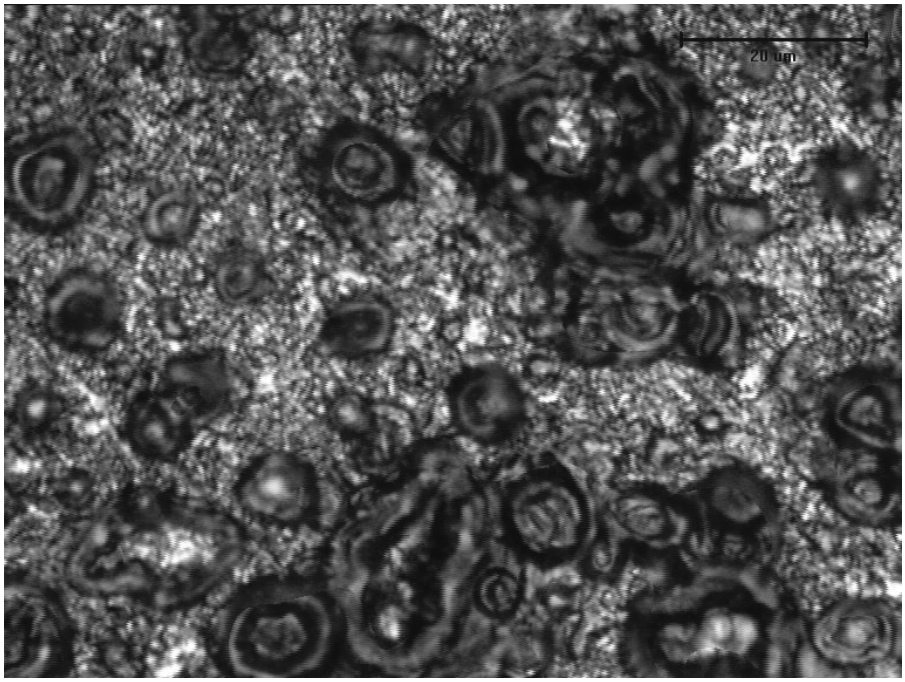

Figure 13 – Appearance of carbon steel surface after long term treatment with TGA formulation. The image shows pit clusters associated with IPRM transient (X50).